# Optimization of a 1×8 Arrayed-Waveguide Grating Multi/Demultiplexer*

OU Hai-yan(欧海燕), LEI Hong-bing(雷红兵),
YANG Qin-qing(杨沁清) and WANG Qi-ming(王启明)

(State Key Laboratory on Integrated Optoelectronics, Institute of Semiconductors,
The Chinese Academy of Sciences, Beijing 100083, China)

HU Xiong-wei(胡雄伟)

(National Research Center of Optoelectronic Technology, Beijing 100083, China)

**Abstract** Using transmission function and diffraction loss function, the crosstalk, diffraction loss and non-uniformity of the 1×8 arrayed-waveguide grating multi/demultiplexer are simulated and values of 2M+1 and width of the tapered waveguide are optimized. The simulation results verify that the device we've designed has high performance.

**Key Words**: Multi/Demultiplexer, Waveguide Grating, Optimization
**EEACC**: 4190, 4130, 4140
**Article ID**: 0253-4177(2000)01-0012-06

## 1 Introduction

The integrated-optical 1×$N$ wavelength multi/demultiplexer, which is based on an arrayed-waveguide grating (AWG DMUX) is the key device in the wavelength division multiplexing (WDM) optical transmission systems[1~5]. The multiplexer is composed of an arrayed-waveguide grating, input-output (I-O) waveguides, and focusing slab waveguides. The arrayed-waveguide grating consists of regular arranged waveguides that join two slabs and the lengths between adjacent waveguides differ from a constant value. The length difference results in the wavelength-dependent wavefront tilting so light convergence in the output slab is wavelength-dependent, and the arrayed waveguide grating operates like a

* Supported by the National Natural Science Foundation of China under Grant No. 69896220, 69889701 and 69876260.

OU Hai-yan(欧海燕) Since 1997, has been working toward Ph. D. and engaged in research on Si-based optical waveguide devices.

WANG Qi-ming(王启明) is an academician of Chinese Academy of Science. His current research interest is in semiconductor optoelectronics, especially in Si-based optoelectronics.

Received 2 July 1999, revised manuscript received 30 August 1999

diffraction grating. The key point is that the arrayed-waveguide grating operates at a high diffraction order, as leads to wavelength resolutions to be better than a nanometer despite its small overall size (of the order of centimeters).

## 2 Transmission Function and Diffraction Efficiency

### 2.1 Transmission Function

The AWG device is considered to be composed of four parts, as is shown in Fig. 1. Part 1 is the input beam propagation in the input waveguide, which ends with an input beam image at the input Rowland circle; part 2 is the phased-array input, i. e. the power collection part, where the input beam diffracts in the slab waveguide and is collected by the grating array; part 3 is the phased grating diffraction, where the beam propagates in each of the grating array waveguides and generates the wavelength-dependent diffraction in the second slab waveguide; and part 4 is the focused image part, where the beam is focused and couples into the output waveguides at the output Rowland circle.

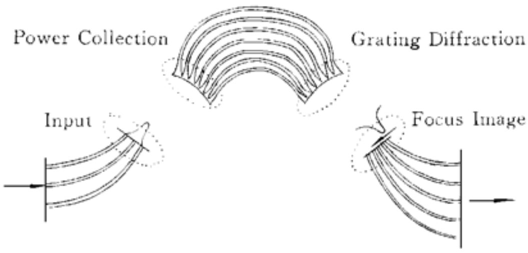


FIG. 1 The Modeling of AWG Structure

The transmission of the optical beam in the device is given as the follows:

$$T = \Bigg| \sum_{j=-M}^{M} \iint \rho_i(x_i) \exp[i2\pi n_s \xi(j, x_i, x_{gi})/\lambda]\, \rho_g(j, x_{gi})\, dx_{gi} dx_i$$

$$\exp\left\{ i \frac{2\pi}{\lambda}[j n_s d(\theta_i + \theta_o) + j(n_c \Delta L + \varphi(j))] \right\}$$

$$\iint \rho_o(x_o) \exp[i2\pi n_s \xi(j, x_o, x_{go})/\lambda]\, \rho_g(j, x_{go})\, dx_{go} dx_o \Bigg|^2 \qquad (1)$$

where $x_{i(o)}$ is the coordinate perpendicular to the waveguide axis at the intersection of the input (or output) and slab waveguide, and $x_{gi(o)}$ is the coordinate perpendicular to the intersection of the input (or output) grating waveguides and slab waveguides. $\rho_i(x_i)$, $\rho_g(j, x_{gi})$, $\rho_o(x_o)$ and $\rho_g(j, x_{go})$ are the field distributions of the mode in an input waveguide, the $j$-th input grating waveguide, output waveguide and the $j$-th output grating waveguide, respectively.

The first integral in Eq. (1) expresses the process in part 1 and 2, where the beam diffracts and is collected by the phased array. The second integral represents the process in part 4, where the image is focused and coupled into the output waveguide's eigenmode. The exponential term represents the process in part 3, i. e. the total phase change produced by the AWG. The $\varphi(j)$ is an effective path length variation in the $j$-th arrayed waveguide, which is caused by material and process variations, such as material index variation, waveguide length variation, electro-optic effect or others. $\xi(j, x_i, x_{gi})$ and $\xi(j, x_o, x_{go})$ are the relative phase terms of the radiation far field from the end of the input mode. If the $\rho_i(x_i)$, $\rho_g(j, x_{gi})$, $\rho_o(x_o)$ and $\rho_g(j, x_{go})$ are replaced by the delta function, Eq. (1) can be written as

$$T = \left| \sum_{j=-M}^{M} \rho_g(j, 0)^2 \exp\left[ i \frac{2\pi}{\lambda}[j n_s d(\theta_i + \theta_o) + j(n_c \Delta L + \varphi(j))]\right] \right|^2 \tag{2}$$

## 2.2 Diffraction Efficiency and Loss Non-Uniformity

The diffracted light exhibits multiple orders by the angle difference $\Delta\theta_m$, where

$$\Delta\theta_m = \frac{\lambda_0}{n_s d} \tag{3}$$

and the light diffracts in a series of directions as shown in Fig. 2 by

$$\Delta\theta_{m\pm i} = i\Delta\theta_m, \ (i = 0, 1, 2, \cdots) \tag{4}$$

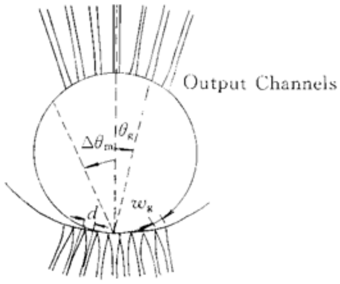


FIG. 2 Diffraction Pattern of the AWG DMUX

where $\Delta\theta_{m\pm i}$ is the diffraction angle of order m $\pm i$. The envelope function of Gauss approximate can be shown as

$$P(\theta) = \exp(-2\theta^2/\theta_g^2) \tag{5}$$

where $\theta$ is the diffraction angle and $\theta_g$, the width of the Gaussian far field, is given by

$$\theta_g = \frac{\lambda_0}{\pi n_s \omega_g} \tag{6}$$

where $\omega_g$ is the half width at $1/e^2$ of the maximum optical power in the channel waveguide with width $w_g$.

Therefore, beam diffraction efficiency is mainly determined by the amount of diffracted lights into the undesired orders, as is given by

$$\eta(\theta) = \frac{P_m}{P_m + P_{m\pm1} + P_{m\pm2} + \cdots}$$
$$= \frac{P(\theta)}{P(\theta) + P(\theta - \Delta\theta_m) + P(\theta + \Delta\theta_m) + P(\theta - 2\Delta\theta_m) + P(\theta + 2\Delta\theta_m) + \cdots} \tag{7}$$

where $P_{m\pm i}$ is the power of order m $\pm i$. By substituting Eqs. (5) and (6) into Eq. (7) as

$$\eta(\theta) = \frac{1}{1 + 2\sum_{i=1}^{\infty}\left[\exp\left[-2\left(\frac{i\Delta\theta_m}{\theta_g}\right)^2\right]\cosh\left(2i\theta\frac{\Delta\theta_m}{\theta_g^2}\right)\right]} \tag{8}$$

The central diffraction efficiency $\eta(0)$ at the central I/O port is defined as:

$$\eta(0) = \frac{P(0)}{P(0) + 2P\left(\frac{\lambda_0}{n_s d}\right) + 2P\left(\frac{2\lambda_0}{n_s d}\right) + \cdots}$$
$$= \frac{1}{1 + 2\exp\left[-2\left(\frac{\pi\omega_0}{d}\right)^2\right] + 2\exp\left[-2\left(\frac{2\pi\omega_0}{d}\right)^2\right] + \cdots} \tag{9}$$

It is found that the diffraction efficiency depends only on the normalized spot size $\omega_0/d$ from Eq. (9).

The diffraction loss, expressed in dB, is given by

$$L_d = -10\log(\eta(\theta)) \tag{10}$$

The maximum loss non-uniformity is $L_{di}$, which is defined by the diffraction loss difference between the central port and the most outer output channel with output angle $\theta_{0,max} \approx N\Delta x_o/(2R)$.

$$L_{di} = -10\log(\eta(\theta_{0,max})) - (-10\log(\eta(0))) \tag{11}$$

## 3 Simulation and Optimization

Table 1 presents the values used for the following simulation and optimization[6].

**Table 1 Designed Values for the Simulation of 1×8 AWG DMUX**

| Symbol | Parameter | Value |
|---|---|---|
| $a$ | The size of square waveguide | 6.1μm |
| $\Delta$ | Relative refractive index difference | 0.75% |
| $N$ | Maximum number of channels | 8 |
| $\lambda_0$ | Center wavelength | 1550.9nm |
| $\Delta\lambda$ | Channel spacing | 1.6nm |
| $\Delta x_i(o)$ | I/O waveguides spacing | 28μm |
| $d$ | Arrayed-waveguide grating pitch | 28μm |
| $n_s$ | Effective index of slab waveguide | 1.452 |
| $n_c$ | Effective index of buried channel waveguide | 1.450 |
| $n_g$ | Group index | 1.496 |
| FSR | Free spectral range | 19.27nm |
| $m$ | Diffraction order | 78 |
| $R$ | Focal length of slab region | 8841.06μm |
| $\Delta L$ | Path length difference | 83.428μm |
| $2M+1$ | Number of array waveguides | 91 |

### 3.1 Transmission Characteristics

Using transmission function Eq.(2) with $P(\theta)$ in Eq.(5) as a relative field in the array waveguides, the spectral response curves of AWG DMUX are shown in Fig. 3 to Fig. 5. Figure 3 shows the relationship of the grating waveguide numbers $2M+1$ versus sidelobes. Enough grating waveguide numbers can suppress the sidelobes and reduce the crosstalk. When $2M+1$ varies from 23, to 43 and 91, the crosstalk varies from −18.26dB to −35.94dB and −83.68dB respectively, so larger $2M+1$ gives better crosstalk performance.

Figure 4 shows the spectral dispersion for the eight channels, where channel spacing $\Delta\lambda$ is 1.6nm, and center wavelength is 1550.9nm. The simulation results coincide with the values we've designed.

The FSR spectra associated with different grating orders are shown in Fig. 5, where FSR= 19.27nm.

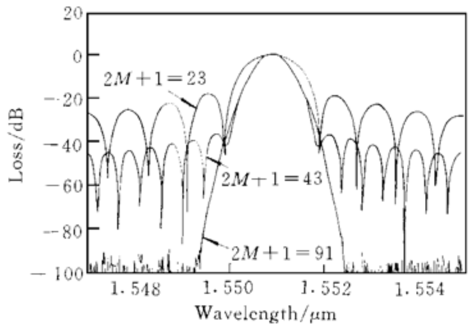


FIG.3　Sidelobes vs. Arrayed-Waveguide Numbers

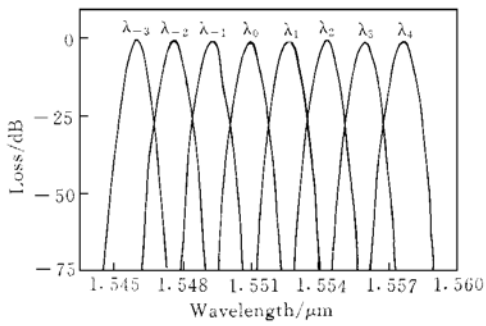


FIG.4　Wavelength Spectrum with 1.6nm Channel Spacing

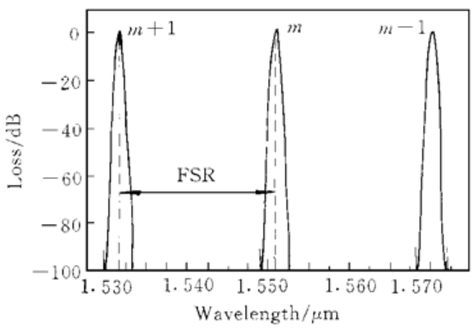


FIG.5　Simulated FSR Characteristics of the AWG DMUX

### 3.2　Diffraction Loss and Non-Uniformity

Figure 6 and 7 shows grating diffraction loss and non-uniformity based on Eqs.(3) to (11). From Fig.6, the widths of tapered arrayed waveguides $w_g$ have important influence on diffraction loss and non-uniformity. When $w_g$ varies from 10μm, to 15μm and 28μm, the central diffraction loss varies from 1.48dB to 0.23dB and $3.1\times10^{-5}$dB, and the non-uniformity varies from 0.76dB to 0.91dB and 0.06dB, respectively. So full tapered arrayed waveguides are preferred to obtain low diffraction loss.

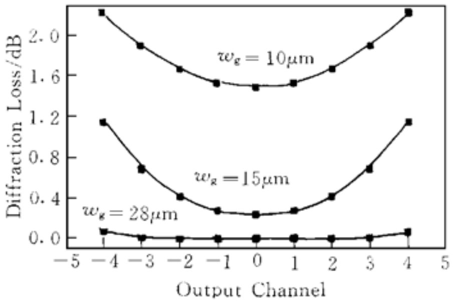


FIG.6　Grating Diffraction Loss of Different Width of Tapered Arrayed Waveguides

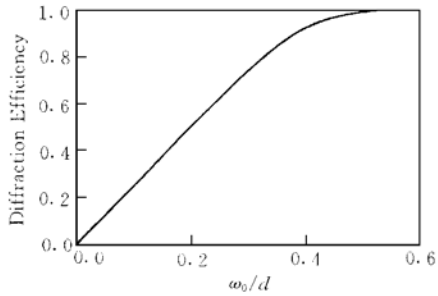


FIG.7　Diffraction Efficiency versus Normalized Spot Size $\omega_0/d$

Figure 7 shows the central channel diffraction efficiency versus normalized spot size. If the grating waveguide is not tapered, substituting $\omega_0$= 4.5μm and $d$= 28μm into Eq.

(9), the largest diffraction efficiency is 0.4 from Fig. 7. So in order to reduce the insert loss and improve the diffraction efficiency, arrayed waveguides should be tapered to increase the normalized spot size $\omega_0/d$.

## 4 Conclusions

Using transmission function and diffraction efficiency equation, we simulated the spectral performance, diffraction loss and non-uniformity of the 1×8 AWG DMUX, and optimized the value of $2M+1$ (the number of grating waveguide) and $w_g$ (the width of tapered grating waveguide). Such conclusions are drawn: the crosstalk, central diffraction loss and non-uniformity are as low as $-83.68$dB, $3.1\times10^{-5}$ dB and 0.06dB, respectively. This verifies that the device we've designed has high performance. Full-tapered grating waveguide is preferred and the value of $2M+1$ should be as large as possible under the permission of processing.

## References

[1] M.K.Smit, Electron. Lett., 1988, **24**: 385~386.

[2] H.Takahashi, S.Suzuki, K.Katoh *et al*., Electron. Lett., 1990, **26**: 87~88.

[3] C.Dragone, IEEE Photon. Technol. Lett., 1991, **3**: 812~815.

[4] C.Dragone, C.A.Edwards and R.C.Kistler, Photon. Technol. Lett., 1991, **3**: 896~899.

[5] H.Takahashi and Y.Hibino, in Dig. 4th Optoelectronics Conf., ICICE, Japan, 1992, Paper 17C1-3.

[6] Ou Haiyan, Lei Hongbing, Yang Qinqing *et al*., Chinese Journal of Semiconductors, to be published(in English).